DOI:10.1002/cnma.202200498
URL: https://onlinelibrary.wiley.com/doi/10.1002/cnma.202200498

Robust, Conformal ZnO Coatings on Fabrics *via* Atmospheric-Pressure Spatial Atomic Layer Deposition with *In-Situ* Thickness Control

Guvanch Gurbandurdyyev[1,2], Kissan Mistry[1,2], Louis-Vincent Delumeau[1,2,], Jhi Yong Loke[1,2,*], Chee Hau Teoh[1,2,*], James Cheon[2,3], Fan Ye[1,2], Prof. Kam Chiu Tam[2,3] and Prof. Kevin P. Musselman[1,2,**]*

1- Department of Mechanical and Mechatronics Engineering, University of Waterloo, 200 University Ave. West, Waterloo, ON, Canada
2- Waterloo Institute for Nanotechnology, 200 University Ave. West, Waterloo, ON, Canada
3- Department of Chemical Engineering, University of Waterloo, 200 University Ave. West, Waterloo, ON, Canada

*These authors contributed equally, ** kevin.musselman@uwaterloo.ca
Homepage: https://uwaterloo.ca/mechanical-mechatronics-engineering/profile/kmusselm
Twitter: @musselman_kevin

Abstract

Zinc oxide (ZnO) is a promising material for functionalization of textiles. It can add a range of functionalities, including UV protection, antimicrobial activity, flame retardancy, hydrophobicity and electrical conductivity. Commercialization of ZnO – coated textiles is still limited due to the cost and challenges related to their manufacture. Moreover, making robust coatings on textiles and measuring their thickness is also challenging. In this work, atmospheric-pressure spatial atomic layer deposition (AP-SALD) systems are utilized for the first time to coat synthetic spun-bond polypropylene (PP) and natural cotton fabrics with ZnO. The coatings are found to be conformal and uniform, forming complete shells around the fabric fibers. The growth rate is measured to be ~0.24 nm/cycle using an *in-situ* reflectance setup and Virtual Interface (VI) model, which enable precise control of the coating thickness. The coatings are shown to provide

UV-protection and render cotton fabric hydrophobic. No damage is observed after washing, linear abrasion, adhesion, twisting and bending tests, indicating that the coatings are robust. Aerosol-penetration tests indicate the coatings do not impact the filtering efficiency of fabrics used in N95 respirators. The results are encouraging for industrialization of the AP-SALD technique for functional textiles.

Introduction

In recent years, surface functionalization of textiles has attracted significant attention from many industries, such as clothing, healthcare, and agriculture. Zinc oxide (ZnO) can add many new properties to textiles, including UV protection, moisture control, photocatalytic self-cleaning, antimicrobial activity, flame retardancy, and electrical conductivity, among others, due to its unique chemical, physical, and optical properties.[1] Furthermore, its low cost and biocompatibility make ZnO suitable for industrial applications.[2]

ZnO has already been incorporated into fabrics using different liquid-phase techniques, such as sol-gel,[3] hydrothermal,[4] sonochemical,[5] and electrodeposition,[6] as well as gas-phase techniques, including spray pyrolysis,[7] atomic layer deposition (ALD), and pulsed laser deposition (PLD).[8] In these works, it has been demonstrated that ZnO enhances photocatalytic self-cleaning,[1,3] antibacterial,[7,8] UV-protection,[9] electrical conductivity,[10] hydrophobicity,[11] and many other properties of fabrics.

Most of the reported coating techniques are designed for lab-scale fabrication and thus, mass-production techniques are still needed. For example, gas-phase techniques are typically slow, have complex setups, and require a vacuum environment, which increases the cost.[12] Liquid-phase techniques come with different drawbacks, such as thickness – control issues and

environmental concerns due to the large amounts of waste generated.[9, 13] Furthermore, it has always been a challenge to measure, and hence control, the thickness of coatings on fabrics. The thickness is commonly estimated by coating a rigid substrate under similar conditions and measuring the thickness, which is unlikely to accurately reflect the fabric coating.[14] In addition, the robustness of coatings against different external forces has rarely been studied and is a critical property for commercialization.

In this work, we coat synthetic, spun-bond polypropylene fabrics, which are used as outer and inner layers in N95 respirators, as well as a natural cotton fabric, with ZnO using an atmospheric-pressure spatial atomic layer deposition (AP-SALD) system. AP-SALD is an emerging technique for rapid, open-air, low-temperature deposition of nanoscale thin films. By spatially separating precursor gases using specially designed reactors, AP-SALD eliminates the slow purge steps and chamber requirements of conventional ALD, making large-area, high-throughput deposition of conformal thin films possible.[15] Successful conformal coating of the fabrics is demonstrated, which produces ZnO shells that completely cover the fabric fibers. The process is demonstrated on a lab-scale AP-SALD system, as well as a pilot-scale AP-SALD system that coats a ~225 cm^2 fabric area. Accurate measurements of the coating thickness are obtained during deposition on a fabric using an *in-situ* reflectance setup and Virtual Interface (VI) model.[16] The robustness of the coatings is tested by washing them in detergent solution and applying different mechanical tests, including linear abrasion, tape adhesion, twisting and bending tests. The effect of the ZnO coating on UV-protection, hydrophobicity and aerosol-penetration properties is also examined. This work highlights the potential for mass manufacturing of functionalized fabrics with robust oxide coatings.

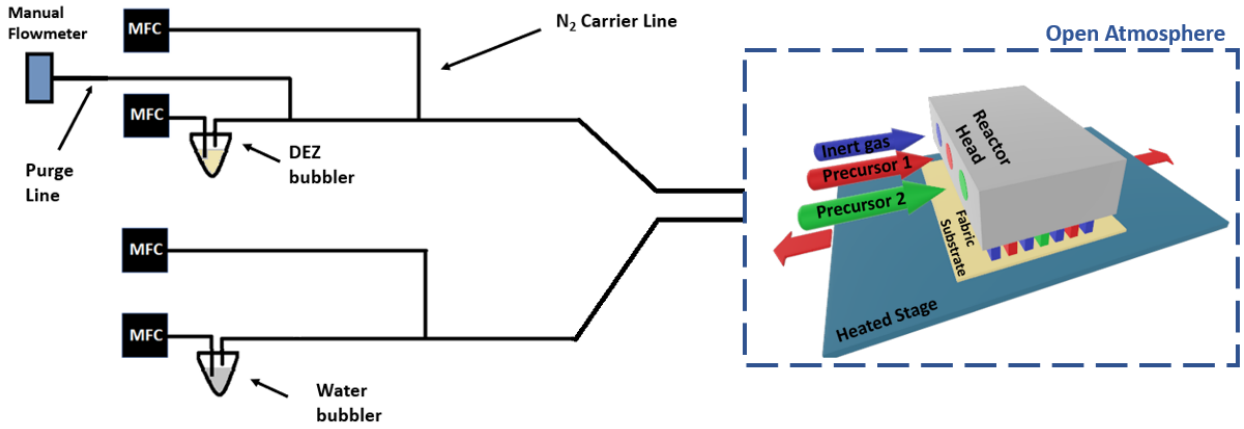

Figure 1. Schematic of the AP-SALD method, including 3D drawing of the reactor head, which shows the continuous flow of the precursors, diethyl zinc (DEZ, green) and water (red).

Results and Discussion

Conformal ZnO Coating of Fabrics by AP-SALD

Pieces of fabric approximately 5 cm x 7 cm in size were first coated with ZnO using a custom-built lab-scale AP-SALD system. A schematic of the AP-SALD system is shown in **Figure 1**. Briefly, nitrogen gas is used to bubble precursors (diethyl zinc and water) and carry their vapors to a reactor head. Parallel gas channels on the bottom of the reactor head deliver the gases to the surface of the fabric. An inert nitrogen gas curtain, as well as exhaust channels, are located between the diethyl zinc (DEZ) and water channels to limit their mixing. The fabric was positioned approximately 100-150 µm underneath the reactor on a heated stage and oscillated back and forth at a speed of 1.5 cm/s. Full details for the depositions are provided in the Experimental Section. In **Figure 2a**, polypropylene (PP) fabric with a density of 50 g/m^2 was taped onto the heated stage by placing a piece of borosilicate glass underneath. This type of fabric is used as the outer layer in N95 respirators. **Figure 2b** shows a piece of the PP fabric with a rectangular area coated at 100 ºC using 100 AP-SALD oscillations. The fabric started to soften at 150 ºC due to the low melting temperature of PP (~160-170 ºC). For that reason, the AP-

SALD was performed at a lower temperature (100 ºC) to conserve the morphology of the fibers. Figure S1 of the Supporting Information shows scanning electron microscopy (SEM) images of uncoated PP fabric fibers, as well as fibers coated with 20 to 100 AP-SALD oscillations. While PP fabric is not conductive, and thus its SEM images were of poor quality due to charging, the conductive ZnO coating facilitated clear SEM images. Importantly, this change in surface conductivity was observed over the entirety of the fabric surface in Figure S1, even after only 20 AP-SALD oscillations, indicating that a conformal, smooth coating was formed, resulting in continuous ZnO shells around the PP fibers. SEM images of PP fabric coated using 100 AP-SALD oscillations are shown in **Figure 2c** and **2d**, which reveal fibers approximately 30 µm in diameter. Energy-dispersive X-ray (EDX) analysis (**Figure 2e**) confirms that there is zinc on the fabric, consistent with the presence of ZnO.

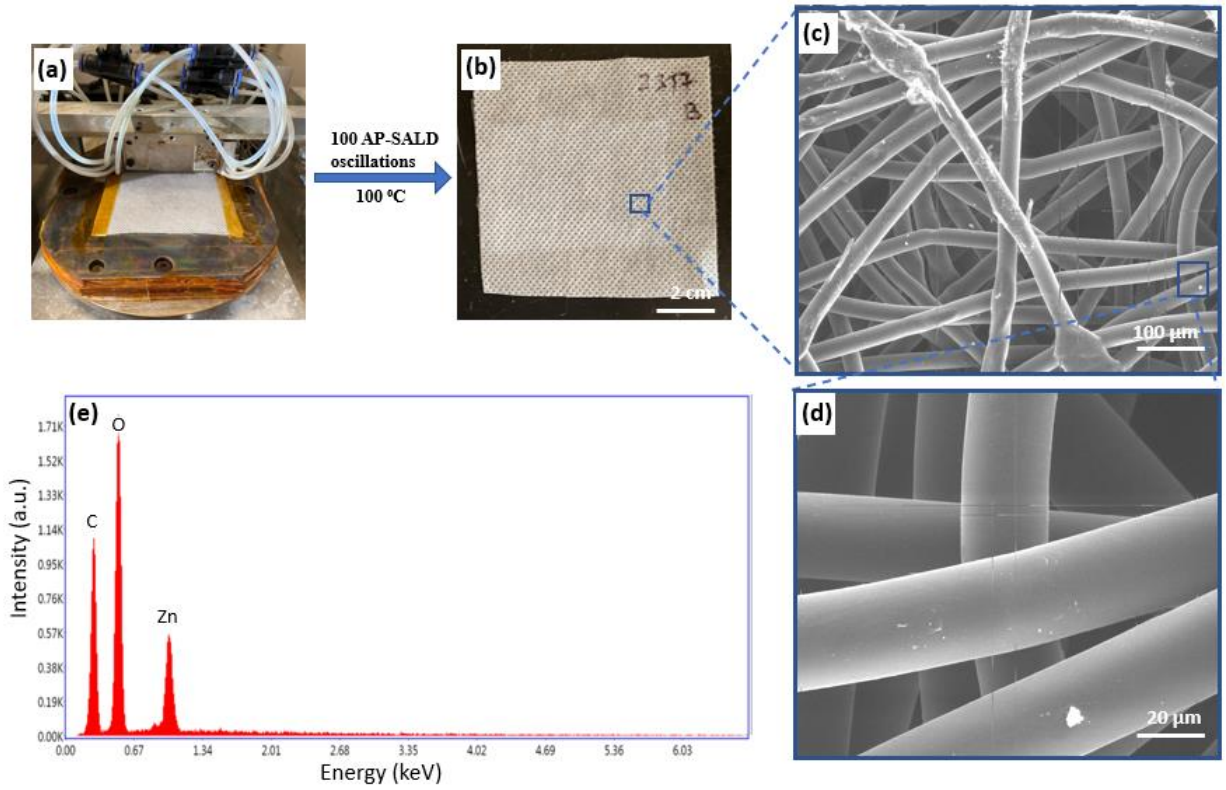

Figure 2. ZnO-coated spun-bond outer polypropylene fabric of N95 respirators (50 g/m^2). (a) PP fabric on heated stage of the AP-SALD system. (b) PP fabric after ZnO coating (100 AP-SALD

oscillations). (c) Low-magnification and (d) high-magnification SEM images of coated PP fabric. (e) EDX spectrum of coated PP fabric.

As mentioned, ZnO can add UV-protective properties to fabrics, particularly in clothing, to protect skin from the harmful effects of UV radiation. The UV-visible absorbance spectrum of the ZnO – coated PP fabric is shown in **Figure 3**. The coated fabric absorbs UV light in the wavelength range of 270 – 380 nm. This corresponds to the UVA and UVB regions of the solar spectrum that are responsible for skin ageing, tanning, and skin cancer (UVC is filtered by the atmosphere and thus, does not reach the Earth's surface).[17] Integrating the UV-protection into clothing fabrics would help to minimize these harmful effects.

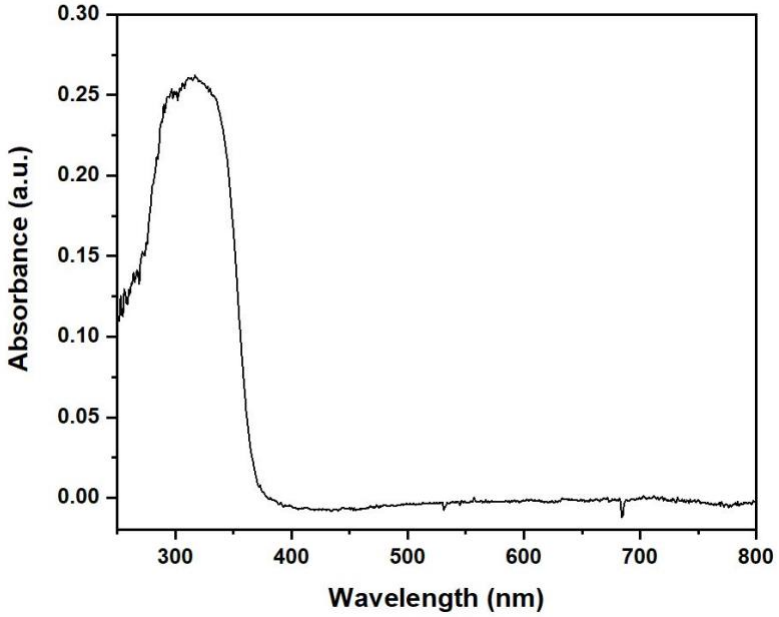

Figure 3. UV-visible spectrum of PP fabric (50 g/m^2) coated at 100 °C with ZnO using 100 AP-SALD oscillations. An identical uncoated PP fabric, which showed negligible absorbance, was used as a baseline for the measurement, and thus the spectrum shown is for the ZnO layer itself.

It is expected that a wide range of textiles could be coated using an AP-SALD system. As a demonstration, two more fabric types were coated with ZnO in an identical manner, as shown in **Figure 4**. Figure 4a shows a SEM image of a spun-bond PP fabric with a lower density (25 g/m^2), which is used as the inner PP layer of N95 respirators. Figure 4c and 4d show SEM

images of a cotton fabric (158 g/m^2) with fiber diameters of approximately 15-20 μm. In both cases, uniform, conformal coatings were again obtained on the fabric fibers. The EDX spectra of these coated PP and cotton fabrics are shown in Figure 4b and 4e, respectively, and again confirmed the introduction of Zn.

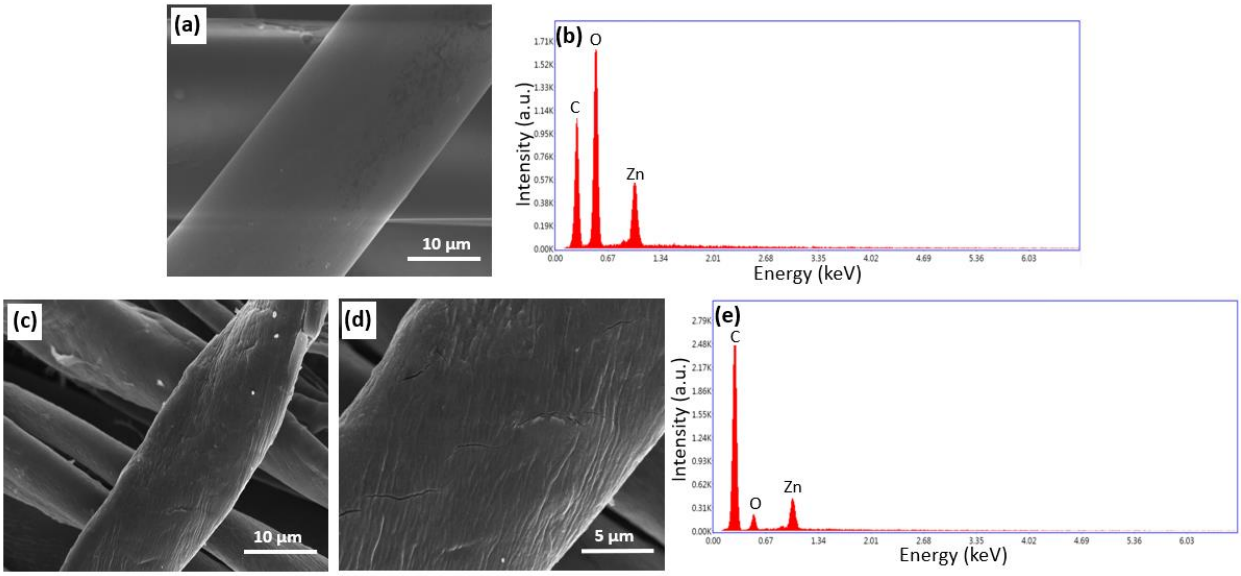

Figure 4. (a) SEM image, and (b) EDX spectrum of ZnO-coated (100 AP-SALD oscillations) inner PP layer (25 g/m^2) of N95 respirators. (c) Lower-magnification and (d) higher-magnification SEM images, and (e) EDX spectrum of ZnO-coated (100 AP-SALD oscillations) cotton fabric.

The formation of continuous shells around the fabric fibers showed a significant effect on water absorbency, especially for the cotton fabric, as has been reported previously for conventional ALD coatings.[18] The cotton fabric is naturally hydrophilic (water contact angle (WCA) ≈ 40º), as shown in **Figure 5a**, but it became highly water repellent after coating it with ZnO (**Figure 5b**). The WCA of a coated fabric was measured to be ~137º. Many reports have shown that the wettability is controlled by surface topography and energy. It has already been shown that the coating roughens the fabric surface at the nanoscale, lowers the surface energy, and increases the fibers' rigidity, which lead to hydrophobicity.[18, 19] In addition, hydroxyl groups on the fiber

surface are consumed to form O – Zn – O bonds, which makes the surface nonpolar, and thus increases the hydrophobicity. The hydrophobic nature of the ZnO coatings can open doors to many new applications in the textile industry.

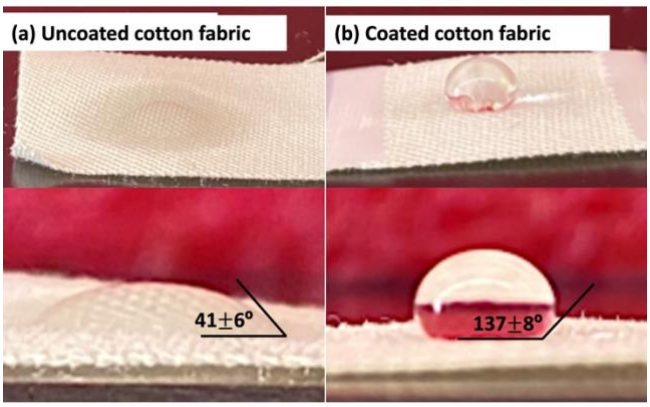

Figure 5. (a) The uncoated cotton fabric absorbed the water droplet, whereas (b) the ZnO-coated cotton fabric (100 AP-SALD oscillations) exhibited water-repellent behavior.

To demonstrate the possibility for scale-up, spun-bond PP fabric (50 g/m^2) was also coated with ZnO using a pilot-scale AP-SALD system designed and built in our lab. This increased the coating area from ~35 cm^2 to ~225 cm^2. The operation of the pilot-scale system was like that of the lab-scale system, with the exception that higher gas flow rates were used (detailed in the Experimental Section). **Figure 6a** shows a 15 cm x 15 cm PP fabric coated at 100 ºC with 650 AP-SALD oscillations (coating area denoted by dashed lines). It is noticeable that the coating is not uniform over the fabric surface due to the fabric not being flat during the deposition, which is a challenge for large areas of fabric. More deposition occurred at the regions where the fabric was bulging downward, where more precursor mixing would have taken place. This would be addressed in a roll-to-roll SALD process with proper tension control. **Figure 6b** and **6c** show SEM images, in which conformal coating of the PP fibers was again observed. Some cracks in the coatings were observed this time, which is likely due to the thicker coating (650 oscillations) deposited using the pilot-scale AP-SALD system compared to the lab-scale depositions (100

oscillations). A thicker coating is expected to result in an accumulation of stress in the film and a greater likelihood of cracking due to applied strain (e.g., unintended flexing of the fabric). In ALD-deposited Al_2O_3 for example, it has been observed that decreasing the thickness of the oxide layer increases the critical strain for crack formation and propagation.[20] **Figure 6d** shows the EDX measurement of the coated fabric; the presence of a zinc peak again confirms the deposition of ZnO.

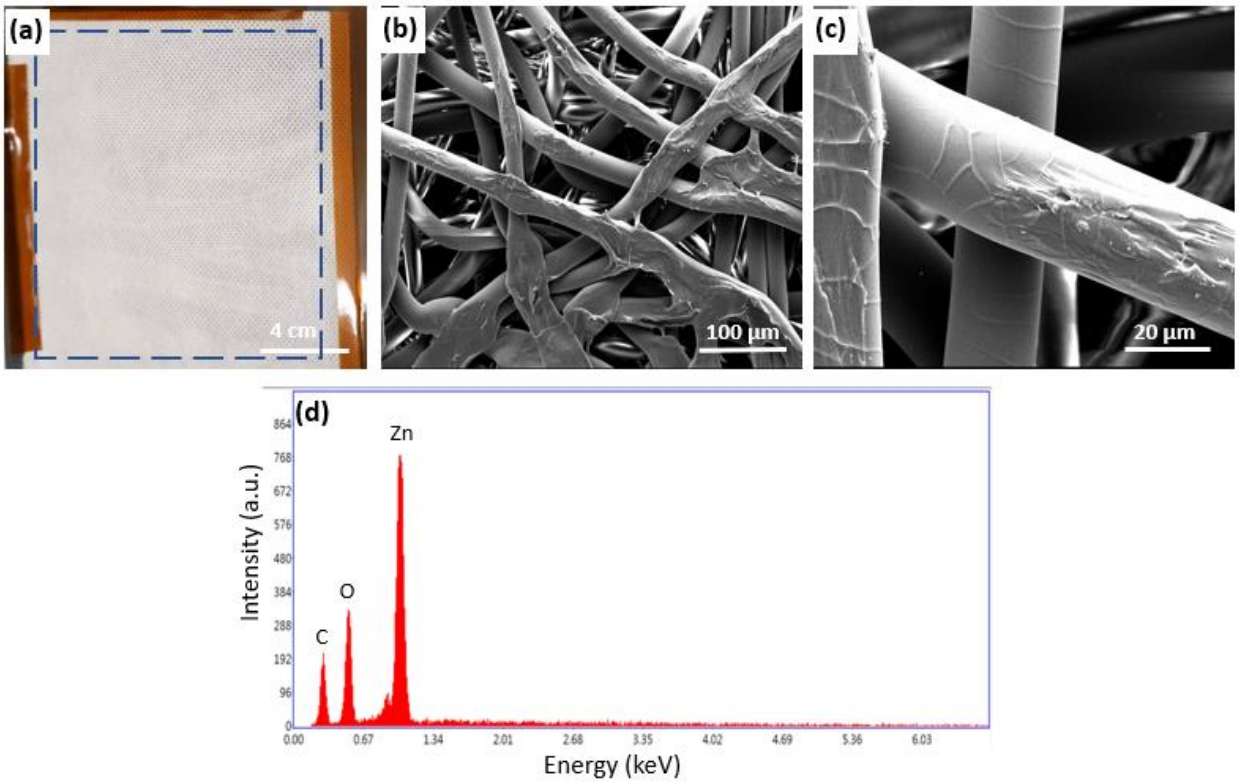

Figure 6. (a) Picture (dashed line spans the coated area), (b) lower-magnification and (c) higher-magnification SEM images, and (d) EDX spectrum of outer PP layer (50 g/m^2) of N95 respirators coated with ZnO (650 AP-SALD oscillations) using a pilot-scale AP-SALD system.

Thickness Estimation by In-Situ Reflectance Measurement and VI Model

The ZnO growth rate and coating thickness were determined by collecting reflectance measurements throughout the deposition and fitting the data to an appropriate model. **Figure 7** shows the *in-situ* reflectance setup used with the lab-scale AP-SALD system in this work. A reflectance probe collected a reflectance spectrum every 10 AP-SALD oscillations (1 AP-SALD oscillation corresponds to 2 ALD cycles, as the substrate moves back and forth underneath the diethylzinc and water). Mistry et. al. used the same *in-situ* reflectance setup and a Fresnel model (which requires the optical properties of the substrate to be known) to study the nucleation and growth of Al_2O_3 and ZnO films deposited on rigid substrates using the same lab-scale AP-SALD system.[21] Unfortunately, this approach is unsuitable for porous, non-uniform fabrics. Instead, a Virtual Interface model,[16] which does not require the optical properties to be known, was used. In the VI model, Equation 1 is used to model the reflectance data at a single wavelength as a function of time (in this case, AP-SALD oscillations), which should give a damped oscillatory pattern, as illustrated in Figure 7.

$$R(t) = \frac{R_\infty - 2\sqrt{R_\infty R_i}e^{-\gamma t}\cos(\delta t - \sigma - \varphi) + R_i e^{-2\gamma t}}{1 - 2\sqrt{R_\infty R_i}e^{-\gamma t}\cos(\delta t - \sigma + \varphi) + R_\infty R_i e^{-2\gamma t}} \qquad \text{(Equation 1)}$$

In Equation 1, *R(t)* is the reflectance intensity as a function of time, σ is a phase of the internal complex reflectance, R_i and R_∞ are the reflectance of the substrate and an infinitely thick film, respectively. Some of the terms in Equation 1 belong to the oscillatory pattern shown in Figure 7; γ is a decay constant (obtained from two extrema R_m and R_{nm} that are separated in time, T_m), δ is a frequency (obtained from the half-period, T, at R_∞), and φ is a phase shift term. The parameters in Equation 1 can be expressed in terms of the refractive index and extinction coefficient of the coating (n, k), the growth rate (G), and wavelength (λ), as reported previously.[16] Hence *R(t)* is dependent on five unknowns, n, k, G, R_i, and σ, and fitting the data

with Equation 1 allows determination of the growth rate, *G*. In addition to determining the growth rate, the nucleation period for film growth can be estimated by identifying the number of AP-SALD oscillations before the oscillatory reflectance pattern starts.

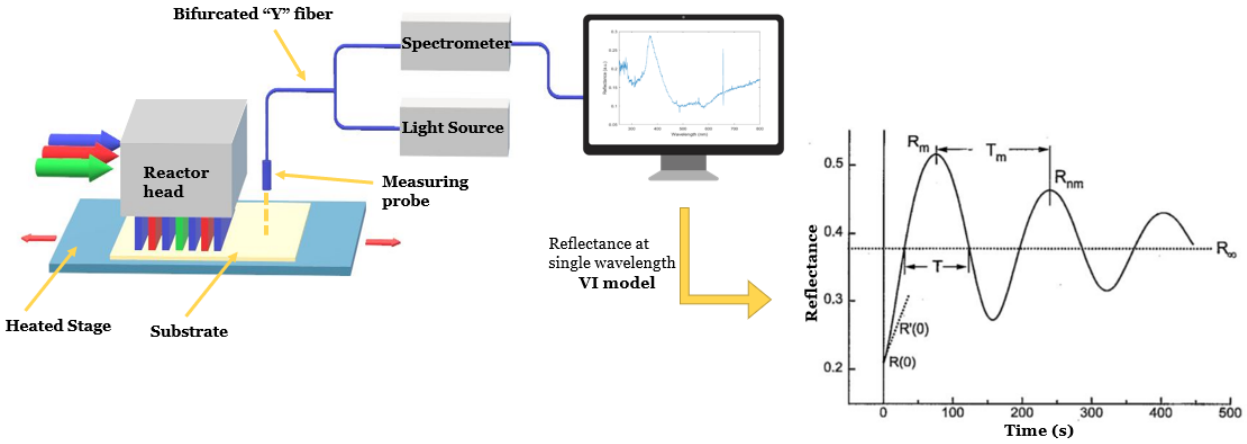

Figure 7. Schematic of the *in-situ* reflectometry setup and the theoretical plot for the VI method that was used to estimate the film growth rate. The oscillatory plot is adapted with permission. [16] Copyright 1995, AIP Publishing.

Figures 8a-d show the reflectance intensity as a function of the number of deposition oscillations at four different wavelengths, measured during the coating of a PP fabric (50 g/m^2) at 100 °C. The reflectance is seen to begin its oscillatory pattern immediately, indicating that the nucleation of the ZnO film on the PP was rapid, consistent with the uniform coating observed on the fabric after 20 AP-SALD oscillations in Figure S1. Different wavelengths were plotted to show the consistency of the obtained growth-per-cycle (GPC) values. To get an accurate fit to the VI model, the measurement must be done until at least two oscillatory periods are observed in the reflectance. The reflectance data at wavelengths lower than 370 nm were found to be too noisy for accurate fitting, and a prohibitively large number of oscillations was required to observe two oscillatory periods for wavelengths higher than 470 nm. For that reason, GPC values were estimated using wavelengths in the range of 370 – 470 nm. Equation 1 was fit to the

oscillatory patterns in Figures 8a-d using a Levengberg-Marquardt nonlinear-least-square fitting method. Good fits to the model ($R^2 > 0.92$) were obtained for all four wavelength and a GPC of 0.24 ± 0.1 nm/cycle was determined for the ZnO deposited on the spun-bond PP at 100 °C. Based on the estimated GPC, the thickness of the ZnO coating on the PP fabric shown in Figure 2 can be estimated as 48 ± 2 nm.

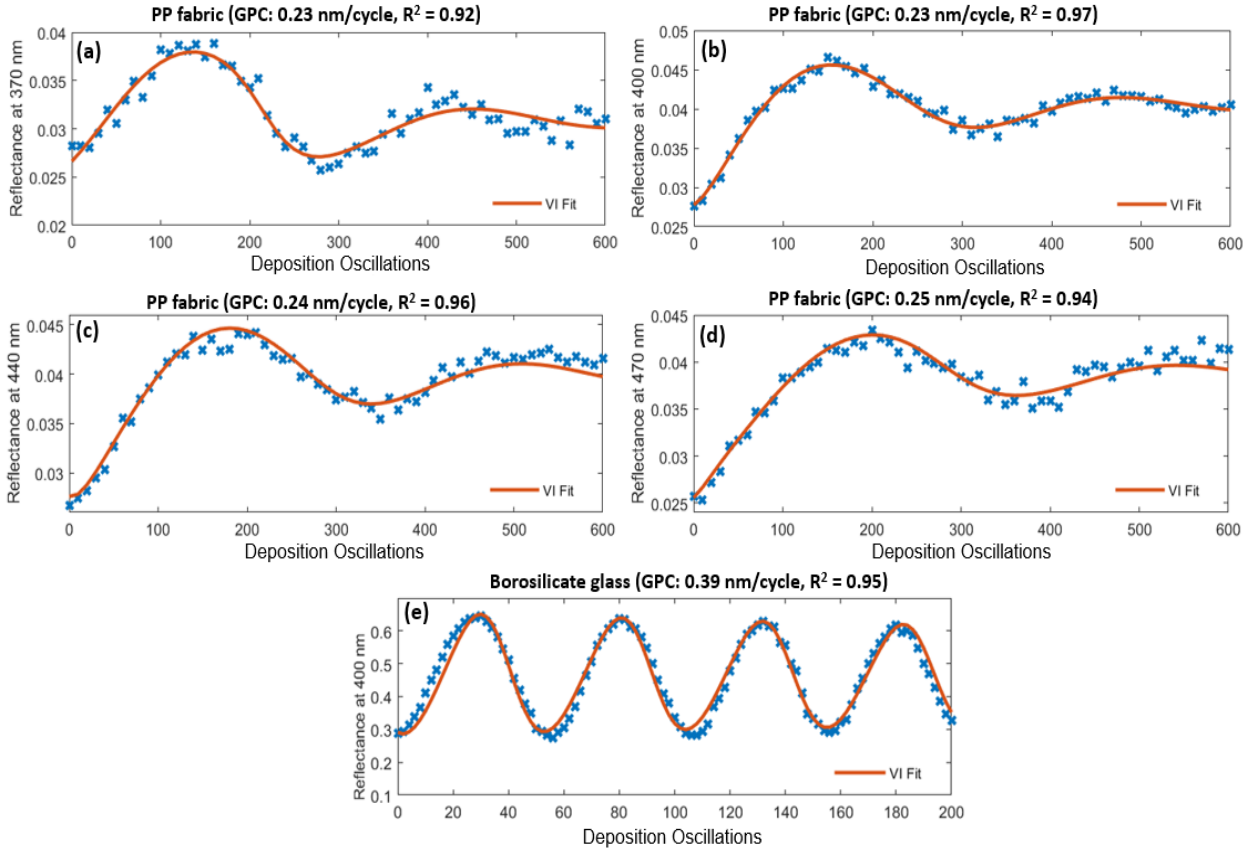

Figure 8. Measured reflectance intensity at (a) λ=370 nm, (b) λ=400 nm, (c) λ=440 nm, and (d) λ=470 nm, as a function of number of deposition oscillations for ZnO films coated on spun-bond PP fabric at 100 °C. (e) Same measurement at λ=400 nm for ZnO coating on borosilicate glass substrate. The plots were fitted to the VI model (red).

It is noted that the GPC of 0.24 ± 0.1 nm/cycle is larger than that typically reported for ALD of ZnO (0.15-0.20 nm/cycle on glass and silicon substrates).[22] In this AP-SALD technique, the experimental parameters (e.g., gap between the substrate and reactor head, gas flow rates,

substrate oscillation speed) must be carefully controlled to ensure that the precursors reach the substrate and react at the surface without mixing in the gas-phase. When gas-phase precursor mixing occurs, chemical vapor deposition (CVD), sometimes referred to as atmospheric-pressure spatial CVD (AP-SCVD), can result. AP-SCVD exhibits a higher growth rate than AP-SALD, while still producing conformal, pinhole-free films.[15, 21] The larger GPC suggests that AP-SCVD may be occurring here. It is possible that the porous nature of the fabric contributes to this, by trapping the diethylzinc and water vapors in the fabric.

For comparison, the same GPC measurement was performed on a borosilicate glass substrate, as shown in **Figure 8e**. Despite using identical deposition conditions as for the fabrics, a larger GPC of 0.39 ± 0.3 nm/cycle was observed for the ZnO on the glass. This is likely due to the different morphologies of the two substrates, which would result in different precursor flow patterns, and clearly demonstrates that it is not accurate to estimate the thickness of a coating on fabric, based on a growth rate measured on another substrate. Hence, the *in-situ* reflectance method demonstrated here is very valuable for precisely controlling the coating thickness on fabrics.

Robustness of Coatings under Various Mechanical Forces

The robustness of the coatings is critical, as the fabrics may be washed and frequently exposed to various mechanical stress during use. Five different tests were performed on PP fabrics (50 g/cm^2) coated with ~48 nm of ZnO to test the coating robustness. These tests included washing in detergent solution, linear abrasion by repeatedly exposing the coated fabric to 180-grit sandpaper, coating adhesion by removing scotch tape from the coated surface, repeatedly twisting the coated fabric 360º, and repeatedly bending the coated fabric around a rod with a 4.5

mm radius (see Experimental Section for full details). Clear differences in the water contact angles of the fabrics were not observed after the tests, indicating that the coatings are robust. Therefore, the effect of each test on the oxide coatings was examined using SEM (**Figure 9**). Minimal damage to the coatings was observed. Figure 9b and 9c show some minor surface damage to the coatings on the uppermost fabric fibers after the abrasion and tape adhesion tests. Some microcracks are observed in the coatings in Figure 9d and 9e after the twisting and bending tests, although the coatings remain intact. These tests suggest that the ZnO coatings robustly adhered onto the PP fabric, which is attributed in part to the fact that the coatings form complete shells around the fabric fibers, making it difficult to remove them from the surface of the fibers.

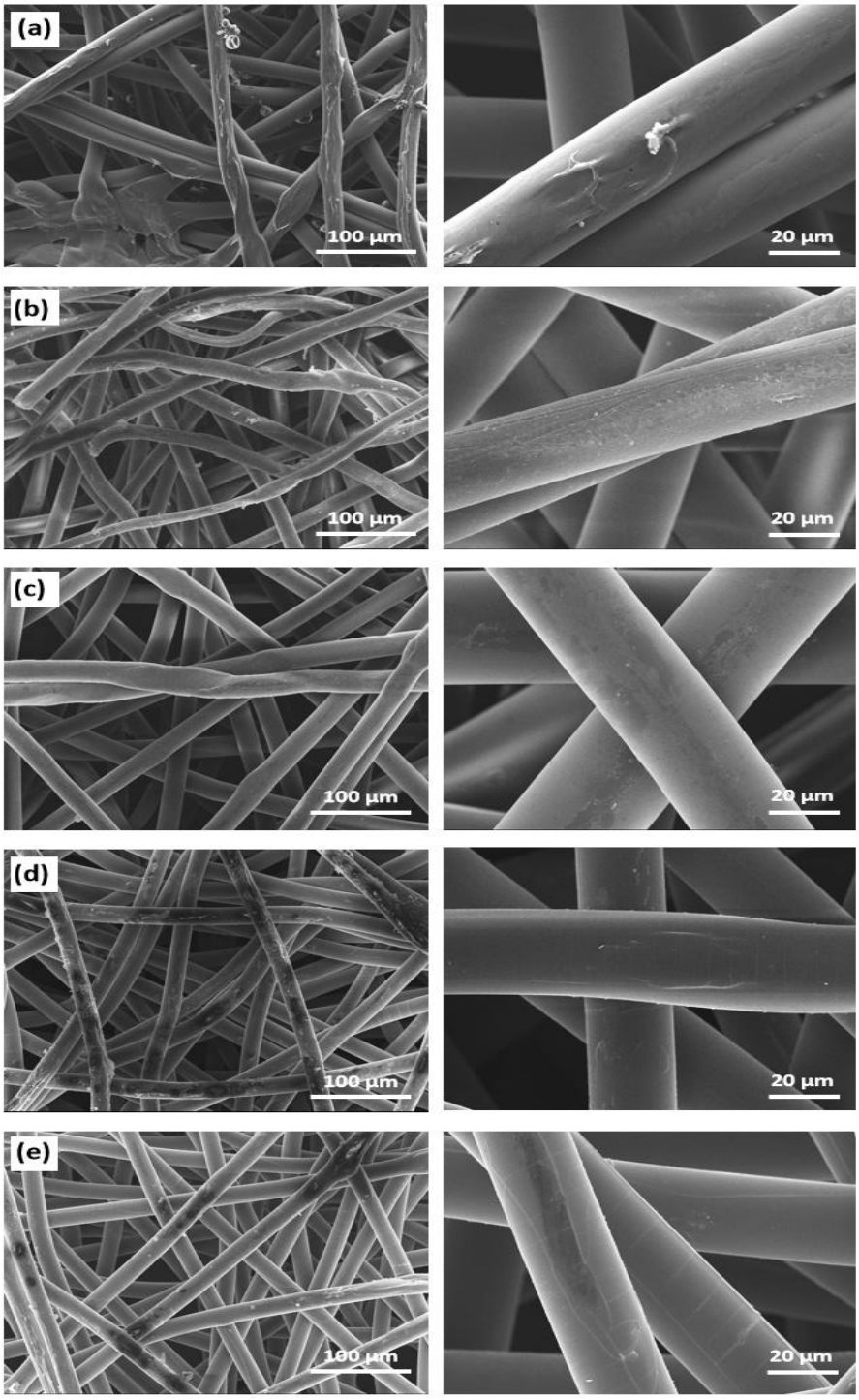

Figure 9. SEM images of ZnO – coated PP fabric after (a) washing, (b) abrasion, (c) tape adhesion, (d) twisting and (e) bending tests.

Effect of Coatings on Aerosol Penetration Performance

For fabrics that could be used in respirator or face-mask applications, such as the PP fabrics studied here, it is important that the coating does not modify the intended aerosol penetration of the fabric. For example, the outer layer of N95 respirators is the part that is contacted most frequently, such as when putting the respirator on, taking it off, and handling it. Applying an antimicrobial coating on the outer layer could help prevent contact-derived infections; however, it would be important to leave the aerosol-penetration properties of the outer layer unchanged, as N95 respirators are designed to trap microbes in interior filter layers. The aerosol-penetration efficiency of the outer spun-bond PP fabric was characterized before and after applying ZnO coatings of various thickness using an 8130A Automated Filter Tester and the established National Institute for Occupational Safety & Health (NIOSH) test procedure, in which the penetration of neutralized NaCl aerosol particles through the fabric is observed.[23] The uncoated PP fabric had a penetration percentage of 92 ± 2%, as shown in **Figure 10**. In other words, its filtration efficiency was only 8%. PP fabrics with ZnO coatings deposited using 50 and 100 lab-scale AP-SALD oscillations, as well as 650 pilot-scale AP-SALD oscillations, had similar penetration percentages within experimental uncertainty. These results clearly demonstrate that coating the PP fabric did not affect the aerosol-penetration efficiency of the fabric.

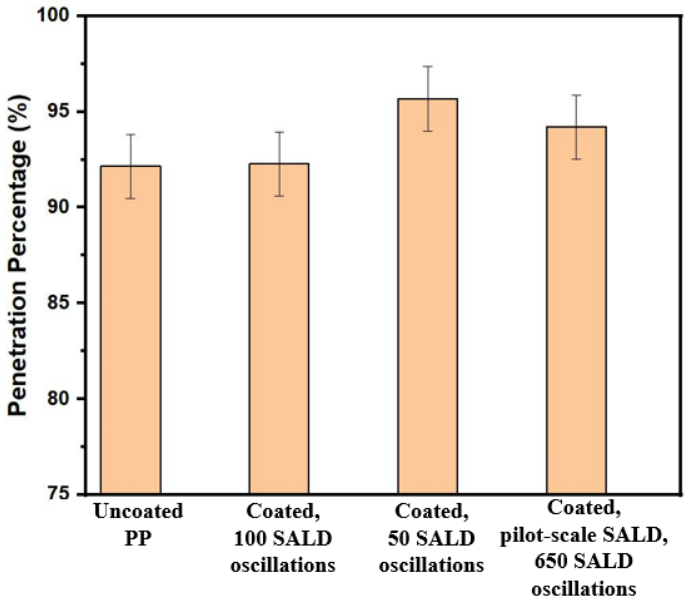

Figure 10. Penetration percentage of uncoated and coated PP fabric (50 g/m^2). A count median diameter of aerosol particle size distribution is 0.075 ± 0.020 μm.

Conclusion

In this work, it has been demonstrated that spun-bond PP and cotton fabrics can be coated with ZnO using an AP-SALD system. The coatings were observed to be extremely uniform and conformal, forming complete nanoscale shells around the fabric fibers. A technique employing *in-situ* reflectometry and a Virtual Interface model was developed to measure the growth rate of the nanoscale coatings on fabric. The GPC of ZnO on the PP fabric was 0.24 ± 0.1 nm/cycle at 100 °C, suggesting that some chemical vapor deposition was likely occurring. Notably, this GPC was different than that observed on a flat borosilicate glass substrate, emphasizing that film growth on other substrates is not an accurate method to estimate film thickness on fabrics. Hence this method is a valuable tool for precisely controlling the coating thickness for functionalized fabrics. The robustness of the coatings was tested using five different mechanical tests: washing, abrasion, tape adhesion, twisting and bending. No significant damage to the coatings was

observed after any of these tests, which is attributed in part to the fact that the coatings form complete shells around the fabric fibers, making them more difficult to remove. The ZnO fabric coating was shown to provide some UV-blocking properties and to alter the wettability of the cotton fabric. Since the spun-bond PP is used as an outer layer for N95 respirators, filter tests were performed and confirmed that the aerosol-penetration efficiency was not affected by the coatings. These conformal ZnO coatings have the potential to be applied to different natural and synthetic fabrics in a range of applications (e.g., personal protective equipment, clothing, linens). Additional AP-SALD process optimization and coating characterization, including accelerated robustness testing building on that reported here, will be needed for this wide range of fabrics and applications

Experimental Section

Deposition of ZnO on Fabric

The coatings were first deposited with a custom-built atmospheric-pressure spatial atomic layer deposition (AP-SALD) system. Inner (25 g/m^2) and outer (50 g/m^2) polypropylene layers of N95 respirators (provided by Eclipse Automation, Canada) and natural cotton fabric (158 g/m^2, sourced from a local fabric store) were cut into 8 cm x 7 cm pieces and taped onto the heated stage (100 ºC) in tension by placing borosilicate glass (7 cm x 7 cm x 0.11 cm, Saida Glass Co.) underneath to avoid deposition on the stage. The depositions were performed by setting the bubbler and carrier gas flow rates to 40 and 210 sccm for DEZ (96%, Fisher Scientific), and 100 and 200 sccm for distilled water. The total flow through the nitrogen-curtain channels was set to 1000 sccm, the gap between the reactor head and substrate was 100-150 μm, and the substrate oscillation speed was 1.5 cm/s.

15 cm x 15 cm sized fabric was coated using a pilot-scale AP-SALD/AP-SCVD system, again using DEZ and H_2O as the precursors. The depositions were performed by setting the bubbler and carrier gas flow rates to 75 and 425 sccm for DEZ (96%, Fisher Scientific), and 240 and 1360 sccm for distilled water. The total flow through the nitrogen-curtain channels was 4800 sccm. The stage was oscillated at a speed of 80 cm/s, with a path length of 11 cm. The stage was maintained at 75°, and the spacing between the reactor head and the fabric substrate was about 750 µm.

In both systems, a vacuum pump was used to remove excess precursors and side-products from the reaction surface via exhaust channels.

Characterization of ZnO Coatings

SEM images and EDX data were collected using a Zeiss Ultra Plus field emission SEM. A Horiba QuantaMaster 8000 spectrometer was used to obtain the UV-Vis absorbance spectra of the samples. An uncoated PP fabric (50 g/m^2) was used as a blank for the absorbance measurement. For the water contact angle measurements, pictures were taken with an iPhone 11 camera and contact angles were measured using ImageJ software.

Estimation of the Growth Rate of Coatings

As shown in Figure 7, a bifurcated reflectance probe (Ocean Optics QR600) was placed perpendicular to the stage. A UV-Visible light source (Ocean Optics DH-2000) sent the light through the probe to illuminate the sample surface and reflected light was collected by a UV-visible spectrometer (Ocean Optics HDX) with a range of 250-800 nm. A reflectance spectrum was collected every 10 AP-SALD oscillations and reflectance at a single wavelength as a function of the number of AP-SALD oscillations was plotted. The collected data was fitted to the

VI model by MATLAB's built-in function "lsqcurvefit", which is a nonlinear least-squares fitting method.

Robustness Tests

For the washing tests, coated fabric samples were washed in 200 mL of water and 1.0 g of laundry detergent ("Gain" Original Liquid) with stirring at 450 rpm for 30 min at 40 °C (Torrey Pines Scientific programmable hot plate HS61). Then, the washed fabrics were rinsed twice within 200 mL of distilled water with stirring for 15 min to get rid of residual detergent particles. Finally, the fabrics were dried at 120 °C for 1 h on a hotplate in air. For the abrasion tests, the fabric was placed face down on sandpaper (180 grit) and a 40 g mass with a contact area of 3.9 cm^2 was placed on top of it. The fabric was moved 10 cm along the sandpaper and then the same process was repeated 15 times. When pulling the fabric, the same angle of ~30° was used for reproducibility. For the twisting tests, one end of the fabric was taped to the edge of a benchtop to keep it stationary. The other end was twisted 360° 50 times in alternating directions. For the tape adhesion tests, the fabric was attached to the surface of a benchtop by taping both ends to keep it static. Scotch tape was placed adhesive side down on the coated fabric and force was applied by placing a 150 g mass with a surface area of 8 cm^2 on the tape for 1 min, after which the tape was peeled off the fabric. The same process was repeated twice for each test. In the bending tests, the fabric was bent around a rod with a radius of 4.5 mm, which was attached to a benchtop. The same area of the fabric was bent then straightened 300 times. After each test, the tested area of the fabric was examined under SEM to observe possible damage.

Filtration Performance

Filter tests were performed to ensure that the coatings developed in this work do not impact the filtering properties of the fabric. An Automated Filter Tester (CERTITEST , Model 8130A, TSI,

Inc.) was utilized to measure the penetration percentage (100% – filtration efficiency) of selected fabrics. Neutralized NaCl aerosol particles were used. The diameter of the equipment's sample holder is 14 cm and thus, a custom sample holder was made from acrylic with an area of 5 cm x 5 cm for the coated fabrics. The flow rate was set to 16.5 L/min to have a face velocity of ~11 cm/s. NIOSH uses an 85 L/min flow rate for a whole face mask,[23] but it was decreased to 16.5 L/min for the smaller test area in this work to keep the face velocity similar. Generated aerosol particles had a size distribution with a count median diameter of 0.075 ± 0.020 μm.

Acknowledgements

The polypropylene fabrics were provided by Eclipse Automation. The authors thank Joe Paquette and Rob Shwery at Eclipse Automation for providing helpful information about the polypropylene fabrics. K.P.M. acknowledges funding from NSERC Alliance (ALLRP 554383-20), NSERC Discovery (RGPIN-2017-04212, RGPAS-2017-507977), Canada Foundation for Innovation John R. Evans Leaders Fund (Project 35552), Canada Foundation for Innovation Exceptional Opportunities Fund COVID-19 (Project 41017), and Ontario Ministry of Research, Innovation and Science Low Carbon Innovation Fund (Project Perovskite Photovoltaics).

Conflict of Interest

The authors declare no conflict of interest.

Keywords: Atmospheric-pressure spatial atomic layer deposition, robust coatings, textiles UV/Vis spectroscopy, zinc oxide.

References

[1] a) M. Shaban, M. Zayed, H. Hamdy, *RSC Adv.* **2017**, *7*, 617; b) N. Jones, B. Ray, K. T. Ranjit, A. C. Manna, *FEMS Microbiol. Lett.* **2008,** *279*, 71; c) R. L. Z. Hoye, K. P. Musselman, J. L. M. Driscoll, *APL Mater*. **2013**, *1*, 060701; d) A. Verbič, M. Gorjanc, B. Simončič, *Coatings* **2019**, 9(9):550.

[2] a) J. Zhou, N. Xu, Z. Wang, *Adv. Mater.* **2006,** *18*, 2432; b) C. Ostrovsky, S. Kazimirsky, G. Gedanken, Brodie, *J. Nano Res.* **2009**, *2*, 882.

[3] H. Sudrajat, *J. Clean. Prod*. **2018**, *172*, 1722.

[4] Z. Zhang, Y. Chen, J. Guo, *Phys. E.* **2019**, *105*, 212.

[5] O. Yayapao, S. Thongtem, A. Phuruangrat, T. Thongtem, *Ceram. Int*, **2013,** *39*, 563.

[6] a) C. Mao, H. Zhang, Z. Lu, *Smart Mater. Struct.* **2017**, *26*, 095033; b) W. T. Chiu, C. Y. Chen, T. F. M. Chang, Y. Tahara, T. Hashimoto, H. Kurosu, M. Sone, *Electrochim. Acta* **2017**, *253*, 39.

[7] a) M. Vasanthi, K. Ravichandran, N. J. Begum, G. Muruganantham, S. Snega, A. Panneerselvam, P. Kavitha, *Superlattice Microstruct.* **2013**, *55*, 180; b) A. G. Cuevas, K. Balangcod, T. Balangcod, A. Jasmin, *Procedia Eng*. **2013**, *68*, 537.

[8] a) R. U. Puvvada, J. P. Wooding, M. C. Bellavia, E. K. McGuinness, T. A. Sulchek, M. D. Losego, *JOM* **2019**, *71*, 178; b) A. J. Karttunen, L. Sarnes, R. Townsend, J. Mikkonen, M. Karppinen, *Adv. Electron. Mater*. **2017**, *3*, 1600459; c) M. C. Popescu, C. Ungureanu, E. Buse, F. Nastase, V. Tucureanu, M. Suchea, S. Draga, M.A. Popescu, *Appl. Surf. Sci*. **2019,** *481*, 1287.

[9] a) G. Broasca, G. Borcia, N. Dumitrascu, N. Vrinceanu, *Appl. Surf. Sci*. **2013,** *279*, 272; b) J. Ran, M. He, W. Li, D. Cheng, X. Wang, *Polymers* **2018**, *10*, 495.

[10] J. S. Jur, W. J. Sweet, C. J. Oldham, G. N. Parsons, *Adv. Funct. Mater*. **2011**, *21*, 1993.

[11] a) G. D. Patil, A. H. Patil, S. A. Jadhav, C. R. Patil, P. S. Patil, *Mater. Lett.* **2019,** *25*, 126562; b) F. H. Kurniawan, P. Chinavinijkul, N. Nasongkla, *J. Drug Deliv. Sci. Technol.* **2021**, *62*, 102339.

[12] R.L. Puurunen, *J. Appl. Phys.* **2005**, *97*, 121301.

[13] a) H. Hu, D. Kremenakova, J. Militký, A. P. Periyasamy, Copper-Coated Textiles for Viruses Dodging (Ch.11) in *Textiles and Their Use in Microbial Protection* (Editors: J. Militký, A.P. Periyasamy, M. Venkataraman) CRC Press **2021**, 235.

[14] a) H. I. Akyildiz, S. Diler, S. Islam, *J. Vac. Sci. Technol., A* **2021,** 39, 022405; b) A. J. Karttunen, L. Sarnes, R. Townsend, J. Mikkonen, M. Karppinen, *Adv. Electron. Mater.* **2017**, 3, 1600459.

[15] a) P. Poodt, D. C. Cameron, E. Dickey, S. M. George, V. Kuznetsov, G. N. Parsons, F. Roozeboom, G. Sundaram and A. Vermeer, *J. Vac. Sci. Technol., A* **2012**, *30*, 010802; b) K. P. Musselman, C. F. Uzoma, M. S. Miller, *Chem. Mater.* **2016**, *28*, 8443; c) K. P. Musselman, D. Muñoz-Rojas, R. L. Z. Hoye, H. Sun, S.-L. Sahonta, E. Croft, M. L. Böhm, C. Ducati, J. L. MacManus-Driscoll, *Nanoscale Horiz*. **2017**, *2*, 110.

[16] W. G. Breiland, K. P. Killeen, *J. Appl. Phys.* **1995,** *78*, 6726.

[17] a) M.T. Landi, A. Baccarelli, R.E. Tarone, A. Pesatori, M.A. Tucker, M. Hedayati, L. Grossman, *J. Natl. Cancer Inst.* **2003**, 94, 94; b) R. M. Halder, C. J. Ara, *Dermatol. Clin*. **2003**, 21, 725; c) B. A. Gilchrest, M. S. Eller, A. C. Geller, M. Yaar, *N. Engl. J. Med.* **1999**, 340, 1341.

[18] a) G. K. Hyde, G. Scarel, J. C. Spagnola, Q. Peng, K. Lee, B. Gong, K. G. Roberts, K. M. Roth, C. A. Hanson, C. K. Devine, S. M. Stewart, D. Hojo, J.-S. Na, J. S. Jur, G. N. Parsons, *Langmuir* **2010**, 26, 2550; b) G. K. Hyde, K. J. Park, S. M. Stewart, J. P. Hinestroza, G. N.

Parsons, *Langmuir* **2007**, 23, 9844; c) A. E. Short, S. V. Pamidi, Z. E. Bloomberg, Y. Li, M. D. Losego, *J. Mater. Res.* **2019**, 34, 563.

[19] a) B. Xu, Z. Cai, *Appl. Surf. Sci.* **2008,** 254, 5899; b) N. Preda, M. Enculescu, I. Zgura, M. Socol, E. Matei, V. Vasilache, I. Enculescu, *Mater. Chem. Phys.* **2013**, 138, 253.

[20] T. O. Kääriäinen, P. Maydannik, D. C. Cameron, K. Lahtinen, P. Johansson, J. Kuusipalo, *Thin Solid Films* **2011**, *519*, 3146.

[21] K. Mistry, A. Jones, M. Kao, T. W. K. Yeow, M. Yavuz, K. P. Musselman, *Nano Express* **2020**, *1*, 010045.

[22] T. Tynell, M. Karppinen, *Semicond. Sci. Technol.* **2014**, 29, 043001.

[23] a) S. Rengasamy, R. Shaffer, B. Williams, S. Smit, *J. Occup. Environ. Hyg.* **2017**, *14*, 92; b) NIOSH: Procedure No. TEB-APR-STP-0059, Revision 2.0. Available at: https://www.cdc.gov/niosh/npptl/stps/pdfs/TEB-APR-STP-0059-508.pdf

Table of Contents

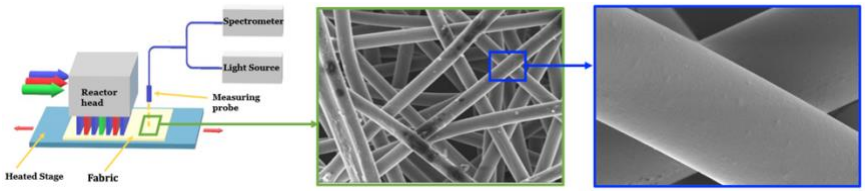

Atmospheric-pressure spatial atomic layer deposition is used to coat polypropylene and cotton fabrics with robust, conformal ZnO coatings that form complete shells around the fabric fibers. An *in-situ* reflectance method enables nanoscale thickness control. The coatings provide UV-protection and hydrophobicity and do not impact the aerosol-penetration efficiency of polypropylene fabrics used in N95 respirators.